Frontiers in Bioscience Landmark

Front. Biosci. (Landmark Ed) **2026**; 31(8): 54167
https://doi.org/10.31083/FBL54167

Original Research

Impact of Resveratrol on Cardiac Remodeling in Female Rats: Emphasizing the Need for Sex-Specific Research

Elizabeth Romero-Monter[1,†], Jazmín Flores-Monroy[1,†], Diego Lezama-Martínez[1], German-Isauro Garrido-Fariña[2], Andrés Aragón-Martínez[3], Ruth-Mery Lopez-Mayorga[4], Karla Reyes-Alvarado[1], Cesar-Froylan Ramirez-Hernandez[1], Diana Ramirez-Hernandez[1,*]

[1]Laboratory of Myocardial Pharmacology, Faculty of Higher Studies Cuautitlán, National Autonomous University of Mexico, 54740 Cuautitlán Izcalli, Mexico
[2]Histology and Biology Support Laboratory, Faculty of Higher Studies Cuautitlán, National Autonomous University of Mexico, 54714 Cuautitlán Izcalli, Mexico
[3]Gamete and Technological Development Laboratory, UBIMED, Faculty of Higher Education Iztacala, 54090 Tlalnepantla de Baz, Mexico
[4]Postgraduate Studies Section, Higher School of Medicine, Instituto Politécnico Nacional, 11340 Mexico City, Mexico
*Correspondence: dramirezhernandez@cuautitlan.unam.mx (Diana Ramirez-Hernandez)
[†]These authors contributed equally.

Academic Editors: Katarzyna Anna Cieslik and Natascia Tiso
Submitted: 23 May 2026 Revised: 14 July 2026 Accepted: 4 August 2026 Published: 25 August 2026

Abstract

Background: Menopause induces estrogen deficiency and promotes a pro-inflammatory and pro-fibrotic cardiovascular environment that increases susceptibility to adverse remodeling after myocardial infarction (MI). This study evaluated resveratrol as an inflammatory modulator and assessed its effects on cardiac fibrosis and hypertrophy in aged ovariectomized Wistar rats with chronic MI. **Methods:** Thirty-six, one-year-old female Wistar rats (450–500 g) were allocated to six groups (n = 6 per group), with or without resveratrol treatment: (1) Sham, (2) Sham-R, (3) Bilateral ovariectomy (OVX), (4) OVX-R, (5) OVX + left anterior descending coronary artery ligation (LADL); OVX-LADL, and (6) OVX-LADL-R. Structural alterations, collagen deposition, and inflammatory profiles were assessed using histological analysis, morphometric measurements, and correlation-based heatmap. LADL in ovariectomized rats resulted in marked structural disorganization, increased cardiac fibrosis, and a predominance of pro-inflammatory mediators. **Results:** Resveratrol treatment attenuated collagen deposition, partially preserved tissue architecture, and shifted the inflammatory profile towards a less pro-fibrotic pattern. Heatmap analysis showed that resveratrol reduced the strength of correlations between inflammatory markers and fibrotic remodeling, particularly in estrogen-deficient animals. **Conclusion:** These findings suggest that resveratrol attenuates adverse cardiac remodeling after MI in ovariectomized rats by modulating inflammation-driven fibrosis under estrogen-deficient conditions a response associated with increased IFN-γ.

Keywords: resveratrol; myocardial infarction; ovariectomy; ventricular remodeling; fibrosis; interferon-gamma; rats, wistar; female

1. Introduction

Sex differences in the development and progression of cardiovascular diseases (CVDs) have received increasing attention, particularly because mortality from myocardial infarction (MI) among women has risen worldwide. Sex-related differences have been reported in genetics and molecular mechanisms involved in hypertrophy, inflammation, fibrosis [1]. In 1984, the NIH first reported that CVDs were more prevalent in women than in men [2]. The risk of MI increases with age and with comorbidities in women, such as hypertension, diabetes, obesity, smoking, and physical inactivity [2]. Age is also a major determinant of MI onset in women, who experience their first MI at an average age of 71 years, compared with 65 years in men [3]. This issue has become relevant as the aged population continues to grow. The increased incidence of MI in older women is thought to be partly related to the loss of the cardioprotective effects of estrogens [2]. Menopause induces cardiometabolic changes that constitute an important CVD risk factor in women [1]. During sex-hormone depletion insulin resistance, increased body mass index, and more inflammatory profile may develop, leading to molecular changes that affect cardiac function and structure. Hormone Replacement therapy (HRT) has been used to address some of these complications; however, not all women are candidates for estrogen treatment. In the 1990s, the Heart and Estrogen/progestin Replacement Study (HERS), which included 2736 postmenopausal women, reported an increased incidence of heart disease and breast cancer associated with estrogen replacement therapy. Between 1990 and 2000, HRT use decreased by 46% in the USA, 28% in Canada, and similar proportions in European countries [4]. Despite extensive efforts to demonstrate the benefits of HRT for postmenopausal changes, its potential risks have limited its use,

supporting the search for alternative therapeutic strategies [5]. Our group previously showed that estrogen depletion induces metabolic changes in the heart that promote remodeling, hypertrophy, and myocardial contractile dysfunction. In that study, early estrogen replacement prevented collagen deposition and reduced ischemic events, although electrocardiographic alterations were observed in the treated groups [6]. One strategy is the use of phytopharmaceutical compounds. Resveratrol was first isolated by Takaoka from Veratrum grandiflorum in 1939 [7]. Since then, it has been widely studied in cancer, inflammation, CVD, and diabetes mellitus [8]. Resveratrol is a polyphenol found in grapes, wine, berries, and peanuts, and has been associated with beneficial effects against oxidative stress, neurodegeneration, inflammation, diabetes, and cancer. The rationale for testing resveratrol in a menopause model is its potential interaction with estrogen signaling. Because of its polyphenolic structure, resveratrol can act as a weak phytoestrogen that interacts with estrogen receptors ERα and ERβ, thereby partially modulating signaling pathways normally regulated by estradiol. This interaction may contribute to restoring nitric oxide (NO) production, reducing vascular inflammation, and improving endothelial function under estrogen-deficient conditions. However, resveratrol has a substantially lower affinity for estrogen receptors than estradiol, suggesting that its effects likely depend on both estrogen receptor activation and independent mechanisms, mainly involving SIRT1 and AMPK. Xin et al. (2010) [9] demonstrated that resveratrol benefited male Sprague-Dawley rats in a model of ventricular stimulation with single, double, and triple extrastimuli by reducing sympathetic neural remodeling, oxidative stress, and inflammatory responses, which may reduce arrhythmias. Feng et al. (2020) [10] reported that resveratrol protected mice against ischemic injury by regulating immune factors such as Sirtuin-1 (SIRT1)/p53 and inhibiting NLRP3-mediated inflammasome activation. Resveratrol also modulates inflammatory pathways involved in cardiovascular pathophysiology. Several studies have shown that it inhibits NF-kappaB activation, decreases the expression of pro-inflammatory cytokines such as TNF-α, IL-1β, and IL-6, and reduces endothelial adhesion molecules, including vascular cell adhesion molecule-1 (VCAM-1) and intercellular adhesion molecule 1 (ICAM-1), which participate in monocyte recruitment during atherosclerosis. In addition, resveratrol activates nuclear factor erythroid 2-related factor 2 (Nrf2), a key regulator of the antioxidant response, thereby increasing cytoprotective genes such as heme oxygenase-1 (HO-1) and NAD(P)H (reduced forms of nicotinamide adenine dinucleotide) quinone oxidoreductase-1 (NQO1). Liu et al. [11] also reported that resveratrol attenuated myocardial injury by inducing KAT5/GPX4 (Lysine Acetyltransferase 5/glutathione peroxidase 4) in the ferroptosis pathway. However, many preclinical studies evaluating the cardioprotective effects of resveratrol have been conducted in male animals [10,12,13]. This highlights the need to evaluate the effects of this polyphenol in aged ovariectomized females and to determine whether estrogen depletion modifies the response to resveratrol. Accordingly, the aim of this study was to evaluate resveratrol as an inflammatory modulator and to assess its impact on cardiac fibrosis and hypertrophy in aged ovariectomized Wistar rats with chronic MI.

2. Methods

2.1. Animals

Thirty-six one-year-old female Wistar rats, weighing 450–500 g, were obtained from the Facultad de Estudios Superiores Cuautitlán, UNAM animal facility. The animals were housed at 24 degrees C under a 12 h light/dark cycle, with free access to food and water. Animal care and experimental procedures were performed in accordance with the Guide for the Care and Use of Laboratory Animals (8th edition, National Academies Press). The project was approved by the Internal Committee for the Care of Experimental Animals of FES Cuautitlán (C22_12) and complied with the Mexican Official Standard NOM-062-ZOO-1999, which establishes technical specifications for the production, care, and use of laboratory animals. The study was carried out in accordance with the ARRIVE guidelines.

2.2 Experimental Protocol

Animals were randomized into six groups (n = 6 per group). Resveratrol treatment is indicated by the suffix ‘R’. The groups were: (1) SHAM-R; (2) SHAM; (3) bilateral ovariectomy with resveratrol treatment (OVX-R); (4) bilateral ovariectomy without resveratrol treatment (OVX); (5) OVX followed by left anterior descending coronary artery ligation for six weeks with resveratrol treatment (OVX-LADL-R); and (6) OVX-LADL without resveratrol treatment (OVX-LADL). LADL groups without ovariectomy were not included because the objective of the study was to evaluate the effect of resveratrol in a menopause-related model. Bilateral ovariectomy was performed to model estrogen depletion. Resveratrol treatment began on the day of ovariectomy. Six weeks after bilateral ovariectomy, LADL was performed and treatment continued for six additional weeks; thus, resveratrol was administered for a total of 12 weeks. Blood pressure was measured using the tail-cuff method, followed by echocardiography under anesthesia with ketamine (35 mg/kg) and xylazine (15 mg/kg) administered intraperitoneally. Animals were then euthanized, and blood and tissue samples were collected. Serum was used to quantify NO metabolites by the Griess reaction and selected pro- and anti-inflammatory cytokines. Hearts and aortas were harvested for histological analysis using Masson’s trichrome and hematoxylin-eosin staining. Infarct area was assessed using 2,3,5-triphenyltetrazolium chloride staining (T8877, Merck, MA, USA).

2.2.1 Resveratrol Treatment

Resveratrol was dispersed in purified water containing 0.5% Poloxamer 407 (Merck, MA, USA). The treatment was administered orally by intragastric gavage at a dose of 33 mg/kg/day for 12 weeks (Best Naturals, premium formula, 500 mg; NJ, USA).

2.2.2 Bilateral Ovariectomy (OVX)

Female rats, one-year-old, were anesthetized with pentobarbital (Sedal-Pharma, Mexico 63mg/mL) administered intraperitoneally at 35 mg/kg. After anesthesia was achieved, the ovaries were exposed through a small incision. The oviduct was ligated and the ovaries were removed. The muscle and skin layers were sutured, and the animals were allowed to recover. Postoperative care included oral gabapentin-tramadol (Aurax, Mexico) at 300/25 mg/kg/day for two weeks. A 6-week recovery period was allowed before LADL [5,6].

2.2.3 Left Anterior Descending Coronary Artery (LADL)

Before surgery, rats were anesthetized with ketamine (100 mg/mL, 35 mg/kg) and xylazine (20mg/mL, 15 mg/kg) administered intraperitoneally (Virbac, Jalisco, Mexico). A thoracotomy was performed between the fourth and fifth intercostal spaces to exteriorize the heart and locate the left anterior descending coronary artery. The artery was ligated using an atraumatic needle and 5/0 silk thread (Atramat, Mexico City, Mexico). The heart was returned to the thoracic cavity, and the muscle and skin layers were sutured. Postoperative analgesia consisted of gabapentin-tramadol (300/25 mg/kg/day, orally) for two weeks. Additional tramadol (6 mg/kg; Aurax, Mexico) was provided in drinking water for two weeks. Animals were allowed to recover for 6 weeks.

Humane endpoints were assessed by continuous monitoring of grooming, food and water intake, and the presence of porphyrin staining, which may indicate pain or distress after surgery. Animals showing these signs were euthanized with an overdose of pentobarbital (63 mg/mL, 100 mg/kg).

Quantification of the Infarct Area. After extraction, hearts were perfused with physiological saline solution, wrapped in Parafilm, and frozen at –20 °C for approximately 1 h. Hearts were then cut into transverse slices approximately 3 mm thick. The slices were placed in a 10 mL Falcon tube containing 1% tetrazolium blue solution and protected from light with aluminum foil. Samples were incubated at 37 °C for 20 min with shaking. The stained tissue was then placed between two glass plates and photographed. Infarct area was quantified using Motic Images Plus 3.0 software (https://www.motic.com/As_microscope_software_r/product_230.html).

2.2.4 Arterial Blood Pressure Measurement

Before post-infarction measurements, rats were acclimatized to restraint for two weeks using the SIEVART1 restraint device in the laboratory and cardboard tubes in the animal facility. Blood pressure was measured in conscious rats using the tail-cuff method. A cuff connected to a computerized oscilloscope was placed on the proximal half of the tail, and measurements were obtained using SPEM equipment and SIEVART version 1 software (Instituto Nacional de Cardiología Ignacio Chavez, Mexico City, Mexico). Mean arterial pressure (MAP) was calculated as follows: MAP = diastolic blood pressure + 1/3 (systolic blood pressure – diastolic blood pressure).

2.2.5 Echocardiography (ECHO)

Before echocardiography, rats were anesthetized with ketamine (35 mg/kg) and xylazine (15 mg/kg) administered intraperitoneally. The anterior chest wall was shaved and cleaned, and ultrasound gel was applied. Echocardiographic evaluation was performed using a SonoScape X5V system (Guangdong, China) in B-mode followed by M-mode.

2.2.6 Quantification of NO by Griess Reaction

Blood samples were collected from each group to quantify serum metabolites of nitric oxide (NO). To reduce nitrate (NO3–) to nitrite (NO2–), VCl3 solution (0.8% in 10% HCl; Merck, MA, USA) was used. Serum proteins were precipitated by adding 100 microL of serum to 200 microL of ethanol:water solution (7:1), followed by centrifugation at 14,500 rpm for 20 min. Then, 100 microL of the supernatant was mixed with 100 microL of VCl3 and 50 microL of sulfanilamide (2% in 10% HCl) in a microtiter plate. After incubation for 20 min at room temperature, absorbance was read at 450 nm.

2.2.7 Histologic Analysis

Hearts were harvested, sectioned transversely into three slices, and fixed in 10% formaldehyde (pH 7.4). Left ventricular samples were formalin-fixed, paraffin-embedded, and cut into 10 micrometre-thick sections using a microtome. Sections were deparaffinized and rehydrated by sequential immersion in xylene, a 1:1 ethanol:xylene mixture, and graded ethanol solutions from 100% to 50%. Samples from the peri-infarct penumbra region were stained with Weigert's hematoxylin or Masson's trichrome for 10 min. Infarct area and collagen deposition were then evaluated.

2.2.7.1 Cardiomyocytes Area Measurement. Cardiomyocyte area was measured in left ventricular sections stained with hematoxylin and eosin. A preliminary microscopic scan was performed using 4× and 10× objectives. Regions containing cardiomyocytes were then identified and examined using the 40× objective. Three fields were captured per

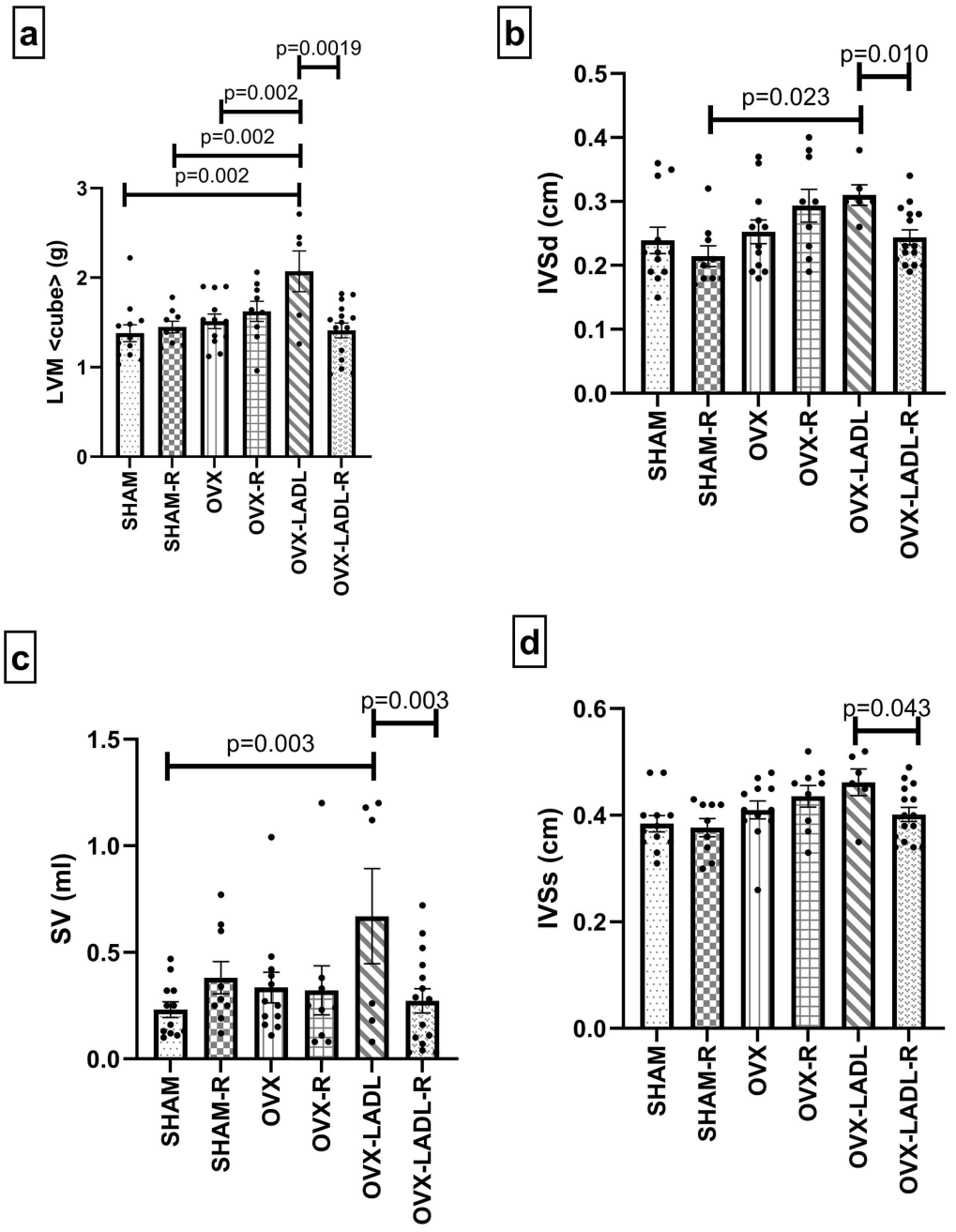

Fig. 1. Echocardiographic parameters. (a) LVM, left ventricular mass; (b) IVSd, interventricular septal thickness at end-diastole; (c) SV, stroke volume; and (d) IVSs, interventricular septal thickness at end-systole. Data are presented as mean ± SEM (n = 6 biological replicates per group; two measurements per animal are displayed individually, resulting in 12 plotted points per group). Statistical analysis was performed using two-way ANOVA followed by Tukey's post hoc test. Horizontal brackets indicate the groups compared; exact *p* values are shown above each bracket. Differences were considered statistically significant at $p < 0.05$.

sample using AmScope software (4.11.20131.20220108, United Scope LLC, Irvine, CA, USA). Six cardiomyocytes were randomly selected from each sample, and their area was measured using Motic Images Plus 3.0 software. Results were expressed in square micrometres. Increased cardiomyocyte area was used as a morphometric indicator of hypertrophy.

2.2.7.2 Quantification of Collagen in the Myocardium. Collagen deposition was measured in left ventricular samples stained with Masson's trichrome. A preliminary microscopic scan was performed to identify regions with the highest collagen content in the free wall of the left ventricle. Three fields were captured from each sample using AmScope software (4.11.20131.20220108). Collagen-positive area was measured using Motic Images Plus 3.0

software. Collagen deposition was expressed as the percentage of collagen-positive tissue relative to total tissue area.

2.2.8 IL-4, IL-10, and IFN-γ Quantification

Serum cytokine concentrations were quantified using a multiplex bead-based flow cytometry assay (Cytometric Bead Array, CBA; BD Biosciences, CA, USA) according to the manufacturer's instructions. Briefly, rat serum samples were diluted (1:4) in assay diluent and incubated with fluorescence-coded capture beads coated with antibodies specific for IFN-γ, IL-10, and IL-4, allowing bead-analyte complexes to form. PE-conjugated detection antibodies were then added to generate sandwich complexes proportional to analyte concentration. After sequential incubations at room temperature and washing steps, samples were acquired on a FACSCanto II flow cytometer using SSC-A for bead discrimination and PE/APC/APC-Cy7 fluorescence channels for analyte detection. Cytokine concentrations were calculated from standard curves generated by serial dilution of recombinant standards using FCAP Array software.

2.2.9 Heat Maps

To explore the relationship between structural remodeling, cardiac function, and inflammatory mediators, Spearman's rank correlation coefficients were calculated among cardiac morphometric variables, echocardiographic parameters, nitric oxide metabolites, and cytokine concentrations. Correlation analyses were performed independently within each experimental group to preserve group-specific association patterns. For each pairwise correlation, the corresponding p value was estimated and adjusted for multiple testing using the false discovery rate method. Missing data were managed by pairwise exclusion.

Group-specific correlation matrices were visualised as heatmaps. Prior to visualisation, variables were scaled to facilitate comparison across parameters with different measurement units. Hierarchical clustering was performed for both rows and columns using Euclidean distance and complete linkage. Heatmaps were generated using R version 4.4.1 and the pheatmap package version 1.0.12. Because this approach is based on correlation analysis, heatmaps were considered exploratory and were not interpreted as evidence of direct mechanistic or causal relationships.

2.2.10 Statistical Analysis

Data are presented as mean ± SEM. The animal was considered the biological experimental unit. For histological and morphometric analyses involving multiple fields or cells per animal, technical measurements were averaged to generate one value per animal before group-level analysis. Normality was assessed using the Shapiro–Wilk test and inspection of residuals; homogeneity of variance was assessed using Levene's or Brown–Forsythe's test.

Primary analyses were performed using two-way ANOVA with experimental condition — Sham, OVX, OVX-LADL — and treatment — vehicle or resveratrol — as fixed factors. When appropriate, a focused 2 × 2 ANOVA was performed in OVX animals using LADL and resveratrol as fixed factors. Interaction terms were reported. Tukey's post-hoc test was used for multiple comparisons when significant main effects or interactions were detected. For non-normally distributed data, equivalent non-parametric or rank-based analyses were applied. A p value < 0.05 was considered statistically significant.

Sample Size Calculation. Sample size was estimated using G*Power [14], considering a confidence level of 95% ($\alpha = 0.05$), statistical power of 86%, an effect size of 0.8, and variability. The test family was F tests, using ANOVA: fixed effects, omnibus, one-way, with an a priori power analysis to calculate the required sample size. The estimated total sample size was N = 28, with a statistical power of 92%. To reduce the number of animals, we also evaluated whether N = 24 would be sufficient; this yielded a statistical power of 86%, which is within an acceptable range for this type of study [15].

3. Results

A significant change in body mass was observed only in the OVX-LADL group, and this change was attenuated by resveratrol treatment. Both the OVX and OVX-R groups showed a numerical reduction in body mass, with a greater decrease observed in the OVX group (−19.12 g) than in the OVX-R group (−6.7 g) (Table 1).

No significant differences in heart weight were detected among groups. Systolic blood pressure (SBP), diastolic blood pressure (DBP), mean arterial pressure (MAP), and heart rate were measured using the tail-cuff method (Table 2). No significant differences were observed in these hemodynamic parameters across groups; however, a non-significant trend towards increased blood pressure was observed in the OVX-LADL group.

Interventricular septal thickness at end-systole and end-diastole increased in the OVX-LADL group (Fig. 1), and these changes were reversed towards normal values by resveratrol treatment. These alterations were associated with increased left ventricular mass in the OVX-LADL group (Fig. 1a). End-systolic and end-diastolic septal thickness were also increased in OVX-LADL animals and were accompanied by increased stroke volume (Fig. 1c).

Table 3 summarizes the echocardiographic parameters measured across experimental groups.

Fig. 2a shows reversal of concentric hypertrophy in the resveratrol-treated groups, together with a trend towards reduced infarct area (Fig. 2b). Myocyte area increased in infarcted animals; however, resveratrol tended to reduce hypertrophy in the ovariectomized infarcted group (Fig. 2c). Collagen deposition increased significantly in OVX-

Table 1. Body and heart mass index.

	GROUP									
Parameter (g)	SHAM	SHAM-R	*p* value	OVX	*p* value	OVX-R	*p* value	OVX-LADL	*p* value	OVX-LADL-R	*p* value
Index mass of heart	0.0028 [0.0024, 0.0035]	0.0030 [0.0028, 0.0035]	0.918	0.0028 [0.0024, 0.0052]	0.87	0.0027 [0.0023, 0.0031]	0.99	0.0029 [0.0024, 0.0035]	0.67	0.0030 [0.0020, 0.0037]	0.75
Δ of corporal mass	–5.45 [–154.7, 72.9]	12.6 [–43.4, 101.0]	0.329	–19.12 [–70.9, 134.7]	0.423	–63.7 [–96.4, –4.9]	0.41	79.4 [17.9, 140.3]	0.029	30.0 [–16.9, 66.7]	0.27

Heart mass index was calculated as heart mass divided by total body mass. Delta body mass was calculated as the final body mass minus the initial body mass after ovariectomy. Data are presented as mean [minimum–maximum] from n = 6 animals per group and were analyzed using Two-way ANOVA. A *p*-value of $p < 0.05$ was considered statistically significant vs sham group.

Table 2. Blood pressure and heart rate.

	GROUP									
Arterial pressure (mmHg)	SHAM	SHAM-R	*p* value	OVX	*p* value	OVX-R	*p* value	OVX-LADL	*p* value	OVX-LADL-R	*p* value
Systolic	143.1 [123.7, 158.0]	145.0 [108.7, 168.0]	0.107	148.5 [142.8, 153.7]	0.107	158.4 [142.3, 170.9]	0.14	159.5 [151.6, 170.9]	0.09	133.6 [106.0, 151.6]	0.54
Diastolic	86.5 [50.1, 118.0]	70.8 [20.7, 105.8]	0.25	94.9 [76.5, 127.3]	0.549	104.4 [60.1, 150.9]	0.74	103.7 [82.2, 138.7]	0.38	90.6 [72.1, 125.8]	0.12
Mean	105.4 [74.6, 131.3]	110.7 [90.3, 125.1]	0.76	112.8 [100.8, 134.0]	0.629	122.4 [91.1, 154.5]	0.59	122.3 [106.0, 149.4]	0.98	106.8 [83.4, 132.2]	0.88
Cardiac frequency (BPM)	235.2 [92.3, 384.61]	126.7 [110.7, 138.56]	0.31	123.1 [73.62, 210.53]	0.307	287.0 [123.45, 555.5]	0.42	251.9 [65.14, 555.5]	0.22	195.6 [46.15, 391.91]	0.67

This table shows mean arterial pressure (MAP), systolic blood pressure (SBP), diastolic blood pressure (DBP), and heart rate values, expressed as mean [minimum–maximum] for n = 6 animals per group. Statistical analysis was performed using Two-way ANOVA.

Table 3. Echocardiographic parameters.

	GROUP									
Parameter	SHAM	SHAM-R	*p* value	OVX	*p* value	OVX-R	*p* value	OVX-LADL	*p* value	OVX-LADL-R	*p* value
LVIDd (cm)	0.46 [0.36,0.59]	0.54 [0.4, 0.71]	0.127	0.52 [0.35, 0.8]	0.09	0.50 [0.32, 0.86]	0.34	0.65 [0.33, 0.93]	0.096	0.47 [0.31, 0.73]	0.21
LVPWd (cm)	0.31 [0.15, 0.52]	0.30 [0.21, 0.44]	1.000	0.30 [0.25, 0.38]	0.94	0.30 [0.15, 0.46]	0.99	0.31 [0.22, 0.43]	0.095	0.30 [0.21, 0.41]	0.96
LVIDs (cm)	0.19 [0.14, 0.24]	0.20 [0.06, 0.39]	0.262	0.19 [0.06, 0.36]	0.33	0.23 [0.06, 0.42]	0.67	0.32 [0.09, 0.59]	0.067	0.20 [0.12, 0.38]	0.39
LVPWs (cm)	0.38 [0.24, 0.57]	0.45 [0.35, 0.61]	0.112	0.48 [0.26, 0.58]	0.46	0.43 [0.32, 0.56]	0.23	0.50 [0.37, 0.65]	0.087	0.41 [0.22, 0.58]	0.093
EDV (mL)	0.25 [0.11, 0.49]	0.42 [0.15, 0.79]	0.383	0.37 [0.11, 1.1]	0.81	0.38 [0.08, 1.38]*	0.0001	0.85 [0.09, 1.68]*	0.020	0.31 [0.07, 0.86]*	0.012
ESV (mL)	0.02 [0.01, 0.04]	0.04 [0, 0.15]*	0.002	0.03 [0, 0.12]*	0.002	0.05 [0, 0.18]*	0.002	0.18 [0, 0.49]*	0.002	0.04 [0, 0.16]*	0.007
EF (%)	90.49 [78.8, 97.19]	91.24 [75.69, 99.73]	0.484	91.01 [58.04, 99.92]	0.27	84.02 [48.78, 99]	0.86	86.30 [71.08, 98.69]	0.47	81.59 [39.91, 99.78]	0.55
CO (L/min)	0.051 [0.02, 0.092]	0.053 [0.014, 0.110]*	0.045	0.035 [0.021, 0.053]	0.08	0.049 [0.017, 0.08]	0.81	0.026 [0.012, 0.038]	0.90	0.063 [0.010, 0.282]	0.86
FS (%)	57.02 [41.56, 70.8]	62.85 [38.75, 86.87]	0.719	64.65 [26.26, 91.23]	0.61	55.61 [20.88, 79.6]	0.65	55.09 [36.17, 77.38]	0.54	54.32 [16.13, 87.8]	0.59
IVS (%)	67.94 [19.12, 133]	77.97 [32.31, 117.5]	0.581	69.63 [4.17, 128.21]	0.087	54.18 [13.41, 98.11]	0.78	51.20 [27.63, 73.77]	0.35	72.19 [0, 134.15]	0.63
LVPW (%)	31.00 [23.3, 62.71]	58.09 [–12.22, 112.77]	0.135	59.18 [3.92, 94.55]	0.24	51.57 [–1.35, 116.6]	0.098	67.71 [50, 87.23]	0.091	41.19 [0, 102.5]	0.39
IVS/LVPW	0.89 [0.39, 2.27]	0.77 [0.42, 1.11]	0.462	0.86 [0.64, 1.47]	0.54	1.00 [0.64, 1.3]	0.37	1.05 [0.72, 1.39]	0.5	0.86 [0.59, 1.3]	0.61

Data are presented as mean [minimum–maximum] (n = 6 animals per group). Statistical analysis was performed using two-way ANOVA followed by Tukey's post hoc test. *$p < 0.05$ versus the Sham group. LVIDd, left ventricular internal diameter at end-diastole; LVPWd, left ventricular posterior wall thickness at end-diastole; EDV, end-diastolic volume; LVIDs, left ventricular internal diameter at end-systole; LVPWs, left ventricular posterior wall thickness at end-systole; ESV, end-systolic volume; EF, ejection fraction; FS, fractional shortening.

LADL animals compared with the Sham ($p = 0.006$), Sham-R ($p = 0.006$), and OVX-R ($p = 0.006$) groups (Fig. 2d,e). Resveratrol treatment reduced collagen deposition in OVX-LADL-R ($p = 0.004$) animals. In addition, myocyte area was lower in OVX animals, whereas LADL increased myocyte size, consistent with infarction-induced hypertrophy. In OVX-LADL-R animals, myocyte area returned towards values comparable to those of non-infarcted groups. The myocardial fiber structure also appeared better preserved in the resveratrol-treated groups (Fig. 2e).

Regarding inflammatory mediators, NO levels decreased in the OVX-LADL-R group compared with the Sham group (Fig. 3a). IFN-γlevels increased significantly in OVX-LADL-R animals, reaching approximately three times the Sham value (Fig. 3b). Resveratrol treatment was also associated with a trend towards increased IL-4 and IL-10 levels (Fig. 3c,d).

Heatmaps in Fig. 4 were constructed to analyze correlations among structural, functional, and inflammatory variables. In the Sham groups, myocyte area was closely associated with NO levels, whereas this relationship was lost in the ovariectomized and infarcted groups. A positive correlation between IFN-γ and left ventricular collagen percentage was observed only in the Sham, Sham-R, and OVX-LADL-R groups, whereas this relationship was absent in the OVX and OVX-R groups. Another relevant positive correlation was observed between NO and IL-4 in resveratrol-treated groups (OVX-R and OVX-LADL-R). In contrast, the OVX-LADL group showed a greater number of positive correlations and a warmer heatmap pattern, whereas the OVX-LADL-R group showed fewer positive correlations.

4. Discussion

In this study, we evaluated the effects of resveratrol, a phytopharmaceutical compound, on adverse cardiac remodeling under estrogen-deficient post-MI conditions. Our findings indicate that resveratrol reduced body mass, helped preserve cardiac output, and improved septal thickness, left ventricular mass, and myocyte area. Resveratrol also reduced NO-related metabolites and was associated with a trend towards reduced infarct area and lower collagen deposition in the left ventricle of OVX-LADL animals. These effects were associated with a selective increase in IFNγ in OVX-LADL-R animals, suggesting that this cytokine may participate in the remodeling response. However, this association should not be interpreted as evidence of causality.

Several molecular mechanisms have been attributed to resveratrol, including inhibition of cell proliferation, modulation of cell-mediated cytotoxicity, and regulation of cytokine production, at least in part through inhibition of NF-kappaB activation [16,17]. Resveratrol also activates Sirtuin-1 (SIRT1), which has been associated with reduced insulin resistance [18].

In the present study, resveratrol reduced body mass. Heatmap analysis also showed that body mass was directly related to cardiac function parameters, including ejection fraction (EF), systolic blood pressure (SBP), and left ventricular mass (LVM). Resveratrol may modulate body mass in OVX rats through at least two mechanisms: reduction of insulin resistance and modulation of the gut microbiota, as reported by Zhou et al. [19] and Wang et al. [20].

During the climacteric and menopausal periods, weight gain is common and has been associated with changes in the gut microbiome [17]. These changes are also linked to reduced metabolism and insulin resistance in women and rodent models, potentially contributing to cardiometabolic disease [21]. Oxidative events during menopause are also associated with both pathological conditions and aging. Although NO contributes to beneficial processes such as endothelial vasodilation, it is also a free radical and weak oxidant whose actions are influenced by its rapid reaction with superoxide. In the present study, resveratrol reduced NO-related metabolites, consistent with Tsai et al. [22], who discovered that resveratrol significantly inhibits NO generation in macrophages by reducing iNOS mRNA expression and protein levels. Similarly, reported by Bi et al. [23] a decrease in nitric oxide and TNF-α levels in microglia. We also observed a direct relationship between NO and body mass only in the OVX-LADL-R group, in agreement with Becerril et al. [24], who described a relationship between NO, leptin, and weight regulation. A positive association between NO and IL-4 was observed only in the resveratrol-treated OVX groups (OVX-R and OVX-LADL-R), consistent with the regulation of NO by resveratrol described by Abolfazli et al. [25]. In addition, resveratrol-associated increases in IL-4 may be relevant to fibrosis modulation, as Yu et al. [26] reported that IL-4-related mechanisms reduced fibrosis in a CCl4-induced liver fibrosis model.

MI is more common in females of advanced age. MI severity is related to infarct size, because ischemia induces cardiomyocyte death and loss of contractile function [3]. During repair, endothelial cells initiate angiogenesis through PI3K/AKT and JAK/STAT pathways [16]. Newly formed capillaries supply nutrients to the infarcted area and support fibroblast differentiation into myofibroblasts [27]. This response contributes to compensation of the injured region. Myofibroblasts activate pathways such as TGF-β, Wnt/β-catenin, Notch, Ras, and RhoA/ROCK, which participate in regeneration, fibrosis, and hypertrophy. In the present study, resveratrol reduced infarct area and collagen deposition in aged ovariectomized female rats with chronic MI. Resveratrol has been shown to modulate SIRT1, PTEN/Akt/Smad2/3, and NF-kappaB pathways associated with myocardial fibrosis [12]. Furthermore, Arafa et al. (2014) [13] showed that, resveratrol treatment attenuated cardiac fibrosis and collagen deposition associated with TGF-β1 signalling in doxorubicin-induced cardiotox-

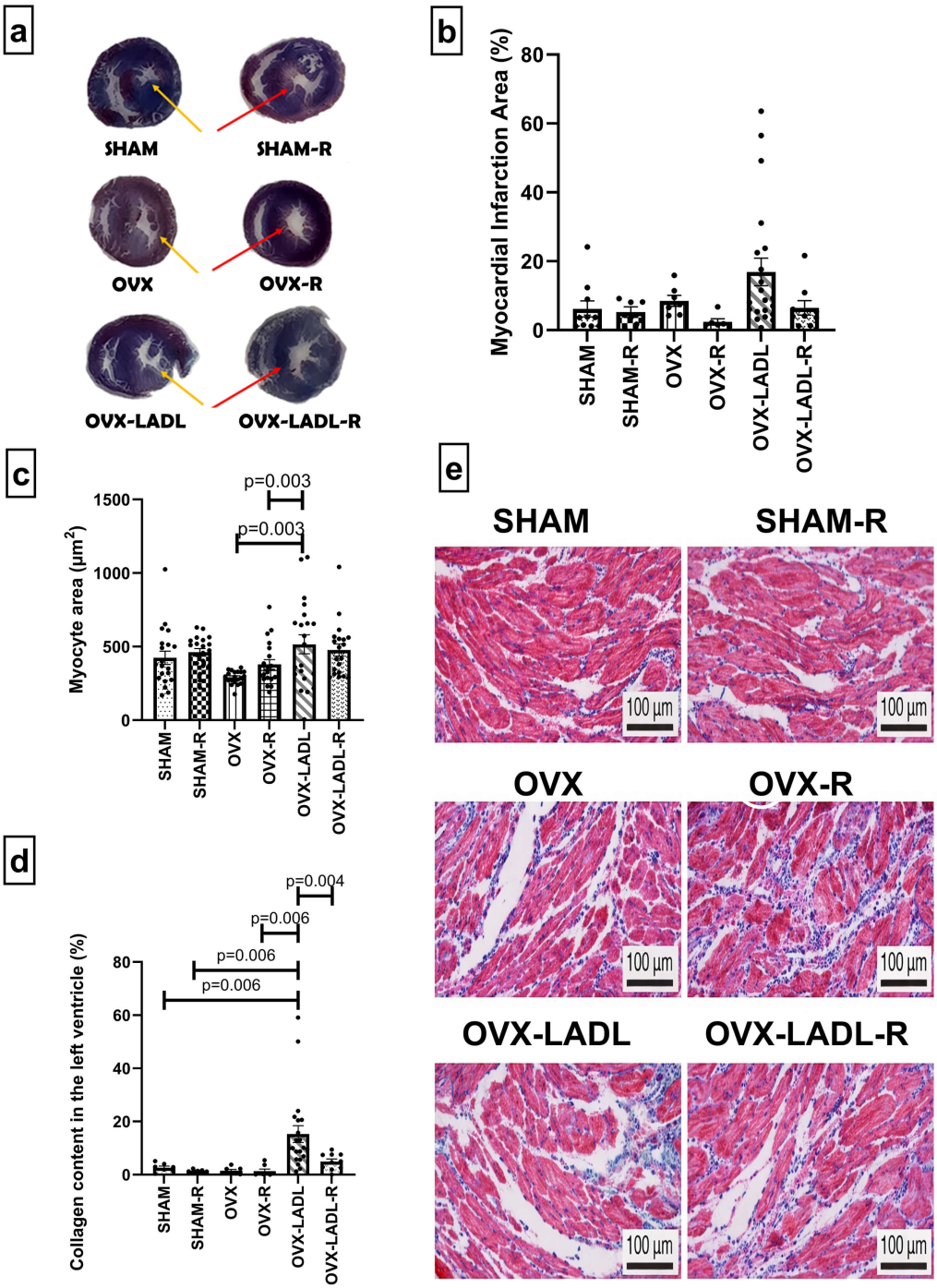

Fig. 2. Collagen deposition. (a) Representative transverse heart sections stained with Masson's trichrome; arrows indicate the left ventricular lumen. (b) Quantification of myocardial infarct area. (c) Cardiomyocyte area. (d) Collagen content in the left ventricle. (e) Representative 40× Masson's trichrome images of the peri-infarct penumbra region. Scale bar: 100 µm. Samples were quantified using Motic Images Plus 3.0. Data are presented as mean +/– SEM (n = 6 biological replicates per group; three measurements per animal are displayed individually, resulting in 18 plotted points per group). Statistical analysis was performed using two-way ANOVA followed by Tukey's post hoc test. Horizontal brackets indicate the groups compared; exact *p* values are shown above each bracket. Differences were considered statistically significant at $p < 0.05$.

icity. We also observed that untreated ovariectomized infarcted rats developed concentric hypertrophy, which was attenuated by resveratrol [13]. Concentric hypertrophy has been associated with sex hormones [28]. Sex-related differences in left ventricular remodeling have been reported in response to pressure overload; in patients with iso-

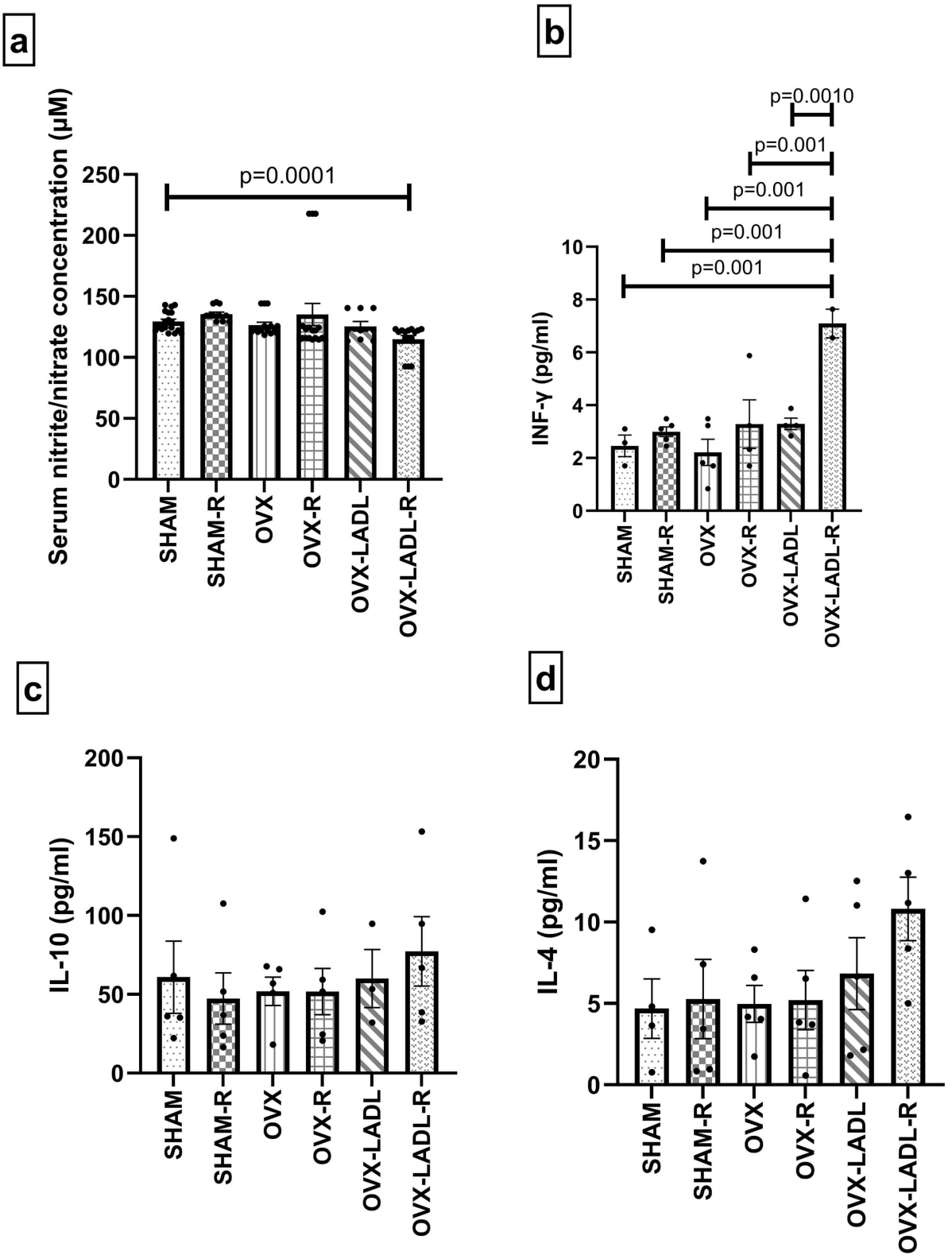

Fig. 3. Inflammatory mediators quantification. (a) Serum nitrate/nitrite concentration as an index of nitric oxide (NO)-related metabolites. (b) IFN-γ concentration. (c) IL-10 concentration. (d) IL-4 concentration. Data are presented as mean +/– SEM (n = 6 animals per group). Statistical analysis was performed using two-way ANOVA followed by Tukey's post hoc test. Horizontal brackets indicate the groups compared; exact *p* values are shown above each bracket. Differences were considered statistically significant at $p < 0.05$.

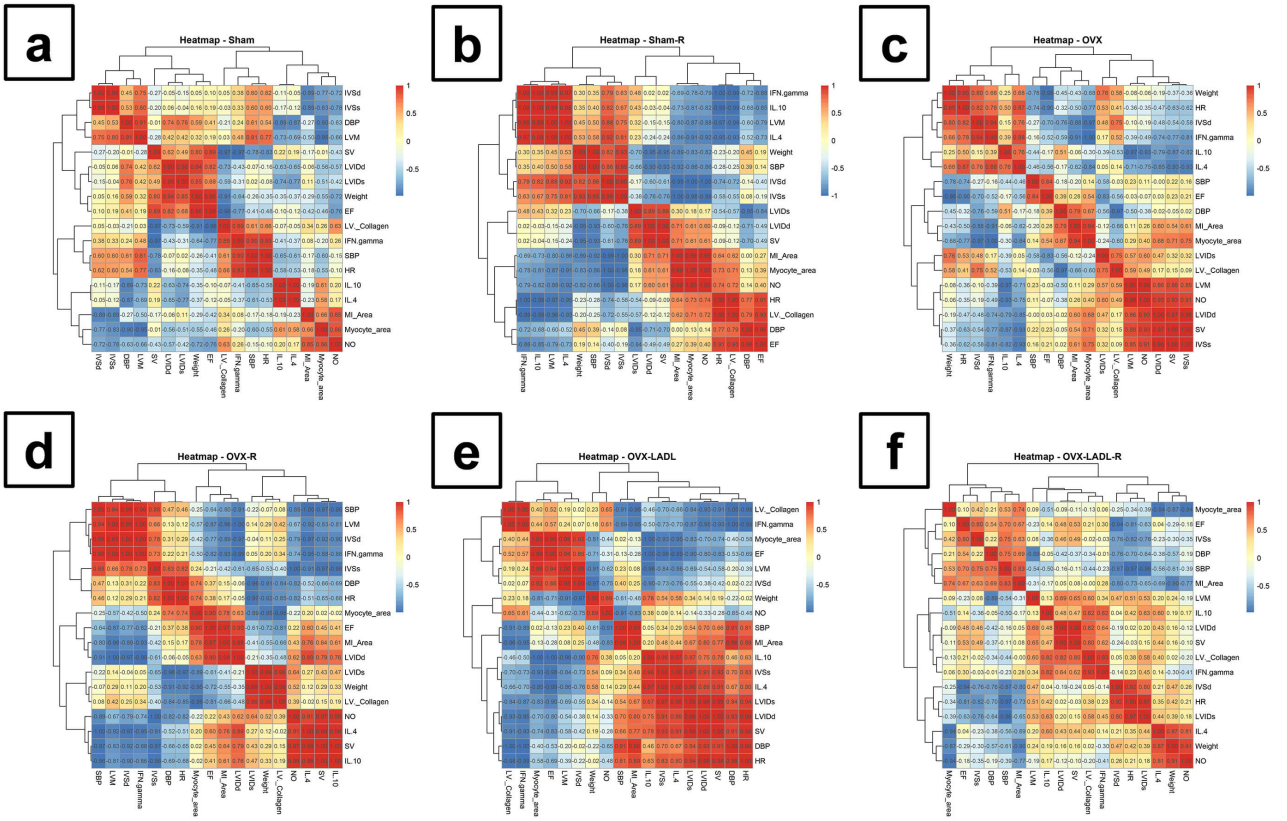

Fig. 4. Heat maps of experimental groups. (a) Sham; (b) Sham-R; (c) OVX; (d) OVX-R; (e) OVX-LADL; and (f) OVX-LADL-R. Red indicates positive correlations between parameters, whereas blue indicates negative correlations. Overall, OVX showed stronger positive correlations than Sham, and myocardial infarction (MI) further increased this pattern. Resveratrol-treated groups showed changes in clustering relationships; notably, the OVX-LADL-R group exhibited reduced heatmap intensity, suggesting weaker correlations among parameters.

lated systolic hypertension, women predominantly exhibited a concentric hypertrophic pattern, whereas men showed an eccentric pattern [29]. These findings may be related to the ability of resveratrol to act as an estrogen mimic. Its stilbene scaffold contains aromatic rings that resemble structural features of 17β-estradiol and diethylstilbestrol, and this effect has been supported by both *in vitro* and *in vivo* studies [30]. Resveratrol interacts with estrogen receptors as a mixed agonist/antagonist [31,32,33], although Kobylka et al. (2022) [30] reported agonistic activity towards ERα and ERβ. Resveratrol has also been reported to modulate IL-2 and IFN-γ and to promote TNF-α production [30]. Although resveratrol treatment reduced collagen deposition in OVX-LADL animals, the present study did not directly evaluate cardiac fibroblast activation or myofibroblast differentiation. Therefore, we cannot conclude that resveratrol directly inhibited fibroblast-to-myofibroblast transition. Future studies should assess α-SMA, periostin, vimentin/DDR2, COL1A1, COL3A1, TGF-β1, p-Smad2/3, MMP2/MMP9, and TIMP1 to determine whether the reduction in collagen deposition reflects direct modulation of fibroblast activation, altered macrophage–fibroblast crosstalk, or secondary improvement of the post-infarction inflammatory environment.

Furthermore, MI triggers an inflammatory response as an adaptive mechanism to ventricular tissue injury. Several studies have demonstrated the immunomodulatory effects of resveratrol both *in vivo* and *in vitro* [17,18,26,34]. In the present study, resveratrol increased IFN-γ levels in aged ovariectomized female rats with MI. This finding should be interpreted cautiously, as resveratrol has been reported to either enhance or suppress IFN-γ depending on dose, cell type, and inflammatory context [35]. IFN-γ has been widely studied in several tumor cell lines, and some studies have demonstrated anti-proliferative and anti-fibrotic effects [36,37] In 2019, Lee et al. [38] showed that co-administration of IFN-γ and 1-methyl tryptophan ameliorated fibrosis in cardiac myofibroblasts by inducing apoptosis through indoleamine 2,3-dioxygenase, resulting in cell-cycle arrest [38]. Based on these observations, the selective increase in IFN-γ observed in OVX-LADL-R animals may be associated with the anti-fibrotic and anti-hypertrophic effects observed in this group. However, the present data do not indicate that resveratrol universally increases IFN-γ

[34]. The increase was observed only in OVX-LADL-R animals, suggesting that this effect is conditional on the combined presence of estrogen deficiency and ischemic myocardial injury. Therefore, in this chronic post-infarction setting, increased IFN-γ should be interpreted not as generalized pro-inflammatory activation, but as a possible component of a remodeling-associated anti-fibrotic response.

Resveratrol was also associated with increased IL-4 and IL-10 levels, both of which are considered anti-inflammatory mediators. The anti-inflammatory effects of resveratrol may involve several mechanisms, including suppression of NF-kappaB and JAK/STAT signaling. Gal et al. (2021) [39] demonstrated that resveratrol can directly inhibit TLR4 expression, thereby attenuating TLR-mediated inflammatory responses and chronic diseases related to TLR activation, including CVD, obesity, and diabetes mellitus [39]. Heatmap correlation analysis revealed strong associations between inflammatory mediators and fibrotic markers in ovariectomized infarcted rats. These correlations were attenuated by resveratrol treatment, suggesting reduced coupling between inflammatory signaling and extracellular matrix deposition. This finding suggests that resveratrol may limit adverse remodeling by attenuating inflammation-fibrosis interactions. Nevertheless, the present findings do not establish whether resveratrol acts through a direct anti-inflammatory mechanism or primarily mitigates the exaggerated inflammatory and pro-fibrotic state generated by the combination of estrogen deficiency and LADL. Both mechanisms are biologically plausible. OVX-LADL likely creates a high-risk inflammatory microenvironment characterized by ischemic injury, damage-associated molecular pattern release, immune-cell recruitment, fibroblast activation, and extracellular matrix deposition. In this context, resveratrol may attenuate adverse remodeling by reducing the coupling between inflammatory signaling and fibrotic remodeling rather than by globally suppressing inflammation. Therefore, the cardioprotective phenotype observed in OVX-LADL-R animals should be interpreted as being associated with modulation of the inflammation-fibrosis axis, not as definitive proof of a direct anti-inflammatory mechanism. Because the study did not include IFN-γ neutralization, receptor blockade, genetic loss-of-function, or direct evaluation of downstream IFN-γ signaling in cardiac tissue, IFN-γ should be considered an associated immunological signal rather than a proven mechanistic driver.

IFN-γ has context-dependent effects in cardiac remodeling. On one hand, it has been reported to exert anti-proliferative and anti-fibrotic effects in cardiac myofibroblast models. On the other hand, IFN-γ can amplify chronic inflammation by promoting macrophage activation, antigen presentation, T-cell recruitment, and STAT-dependent inflammatory gene expression [40]. Thus, in the present chronic post-infarction setting, the selective increase in IFN-γ in OVX-LADL-R animals may reflect a reparative, compensatory, or remodeling-associated immune response. Future studies using IFN-γ neutralization or loss-of-function models are required to determine whether IFN-γ is necessary for the anti-fibrotic effect of resveratrol.

Resveratrol may also attenuate inflammatory responses through estrogen receptor-related mechanisms and SIRT1 upregulation. Fan et al. (2022) [41] reported that resveratrol inhibits RelA acetylation and negatively regulates inflammatory mediators through SIRT1 activation. Jo et al. (2022) [42] showed that resveratrol inhibits M1 macrophage polarization and increases M2 marker expression through the VEGFB/AMPK/NF-kappaB pathway, thereby exerting anti-inflammatory effects and inhibiting cardiac remodeling. Resveratrol may also interfere with TLR4/NF-kappaB and STAT signaling through SIRT1, reducing the release of pro-inflammatory mediators secreted by macrophages and mast cells, including platelet-activating factor, TNF-α, and histamine [42].

While the present study provides evidence for beneficial effects of resveratrol, some limitations should be acknowledged. Although inflammatory markers were evaluated, direct interrogation of specific signaling pathways was beyond the scope of this work. Finally, the experimental design does not allow direct extrapolation to clinical settings, and the doses and timing of resveratrol administration may influence the magnitude of its effects.

5. Conclusion

Estrogen deficiency aggravated post-infarction cardiac fibrosis and adverse remodeling. Resveratrol treatment was associated with reduced collagen deposition, partial preservation of myocardial architecture, improved remodeling-related parameters, and a selective increase in IFN-γ in OVX-LADL-R animals. These findings suggest that resveratrol modulates the inflammation–fibrosis axis under estrogen-deficient post-MI conditions. However, the role of IFN-γ remains correlative and requires functional validation. These findings underscore the relevance of sex-specific approaches in cardiovascular research and support further investigation of resveratrol based interventions in postmenopausal cardiovascular disease.

6. Limitations of the Study

This study has several limitations that should be considered when interpreting the results. First, although resveratrol treatment was associated with reduced collagen deposition and increased serum IFN-γ in OVX-LADL-R animals, the study does not demonstrate that IFN-γ is necessary or sufficient for the observed anti-fibrotic effects. IFN-γ neutralisation, receptor blockade, loss-of-function approaches, and assessment of downstream IFN-γ signalling in cardiac tissue, such as STAT1 phosphorylation, IRF1, or SOCS1, were not performed. Therefore, the role of IFN-γ should be interpreted as correlative rather than causal.

Second, the inflammatory profile was assessed using a restricted panel of mediators. Although IFN-γ, IL-4, IL-10, and NO-related metabolites provide information about selected immune pathways, major post-infarction inflammatory and fibrotic mediators, including IL-1β, TNF-α, IL-6, IL-18, MCP-1, and TGF-β1, were not comprehensively evaluated. In addition, cytokines were measured only at the terminal time point, limiting interpretation of the temporal inflammatory response.

Third, direct markers of cardiac fibroblast activation and myofibroblast differentiation, such as α-SMA, periostin, COL1A1, COL3A1, TGF-β1, p-Smad2/3, MMPs, and TIMPs, were not assessed. Thus, the reduction in collagen deposition cannot be attributed specifically to direct modulation of fibroblast activity. Additionally, the study did not include LADL groups without ovariectomy, which limits the ability to separate the independent effects of myocardial infarction and estrogen depletion on the response to resveratrol.

Finally, some methodological aspects may affect interpretation. Echocardiography was performed using the SonoScape X5V system, which is not an ultra-high-frequency platform specifically designed for small rodents and may affect the estimation of ventricular dimensions and ejection fraction. Heart weight-to-tibia length ratio was not determined, limiting hypertrophy assessment. Plasma or myocardial resveratrol concentrations and pharmacodynamic target engagement were also not measured. Therefore, future studies should include pharmacokinetic analysis, dose-response evaluation, and direct molecular validation of inflammatory and fibrotic pathways.

Availability of Data and Materials

The data that support the findings of this study are available from the corresponding author upon reasonable request.

Author Contributions

ERM, JFM, DRH, and DLM contributed to the design, implementation of the research, and supervised the project. CFRH and KRA participated in experiments. GIGF contributed with the histological analysis. RMLM and AAM contributed to the analysis of the results and to the writing of the manuscript. All authors contributed to editorial changes in the manuscript. All authors read and approved the final manuscript. All authors have participated sufficiently in the work and agreed to be accountable for all aspects of the work.

Ethics Approval and Consent to Participate

The care and use of the animals were conducted in strict accordance with the Guide for the Care and Use of Laboratory Animals (8th edition, National Academies Press). This project was carried out under the authorization of the Internal Committee for the Care of Experimental Animals of FES Cuautitlán (C22_12) and complied with the Mexican Official Standard (NOM-062-ZOO-1999), which sets the technical specifications for the production, care, and use of laboratory animals. The study was carried out in accordance with the ARRIVE guidelines.

Acknowledgment

The authors thank M.C. Crisoforo Mercado Marquez for his support at the FES Cuautitlan animal facility.

Funding

Research carried out thanks to the UNAM program PAPIIT IN204925, UNAM PAPIIT IA204924, Cátedras de investigación FESC CI2211, Cátedras de investigación FESC CI2625. Facultad de Estudios Superiores Cuautitlán, Universidad Nacional Autónoma de México (UNAM), through the Programa Interno de Apoyo para Proyectos de Innovación y Mejoramiento de la Enseñanza (PIAPIME), grant number: PIAPIME 2.11.21.24.

Conflicts of Interest

The authors declared no potential conflicts of interest with respect to the research, authorship, and/or publication of this article.

Declaration of AI and AI-Assisted Technologies in the Writing Process

AI (ChatGPT, OpenAI, version GPT-5.6 Sol) was used to correct the English language, including spelling and grammar checking, and to assist in the preparation of the graphical abstract. After using this tool, the authors reviewed and edited the content as needed and take full responsibility for the content of the publication.

Supplementary Material

Supplementary material associated with this article can be found, in the online version, at https://doi.org/10.31083/FBL54167.

References

[1] Liccardo D, Arosio B, Corbi G, Cannavo A. Sex/Gender- and Age-Related Differences in β-Adrenergic Receptor Signaling in Cardiovascular Diseases. Journal of Clinical Medicine. 2022; 11: 4280. https://doi.org/10.3390/jcm11154280

[2] Mehta LS, Beckie TM, DeVon HA, Grines CL, Krumholz HM, Johnson MN, et al. Acute Myocardial Infarction in Women: A Scientific Statement From the American Heart Association. Circulation. 2016; 133: 916–947. https://doi.org/10.1161/CIR.0000000000000351

[3] Flora GD, Nayak MK. A Brief Review of Cardiovascular Diseases, Associated Risk Factors and Current Treatment Regimes. Current Pharmaceutical Design. 2019; 25: 4063–4084. https://doi.org/10.2174/1381612825666190925163827

[4] Cagnacci A, Venier M. The Controversial History of Hormone Replacement Therapy. Medicina (Kaunas, Lithuania). 2019; 55: 602. https://doi.org/10.3390/medicina55090602

[5] Ramírez-Hernández D, López-Sanchez P, Lezama-Martínez D, Pérez-García E, Montoya-Hernández MFS, Aranda-Fraustro A, et al. Early Estrogen Replacement Therapy Attenuates Cardiac Dysfunction Caused by Aging and Ovariectomy in Female Wistar Rats. Frontiers in Bioscience (Landmark Edition). 2024; 29: 46. https://doi.org/10.31083/j.fbl2901046

[6] Ramírez-Hernández D, López-Sanchez P, Rosales-Hernández MC, Fonseca-Coronado S, Flores-Monroy J. Estrous cycle phase affects myocardial infarction through reactive oxygen species and nitric oxide. Frontiers in Bioscience (Landmark Edition). 2021; 26: 1434–1443. https://doi.org/10.52586/5037

[7] Pezzuto JM. Resveratrol: Twenty Years of Growth, Development and Controversy. Biomolecules & Therapeutics. 2019; 27: 1–14. https://doi.org/10.4062/biomolther.2018.176

[8] Bhat KP, Lantvit D, Christov K, Mehta RG, Moon RC, Pezzuto JM. Estrogenic and antiestrogenic properties of resveratrol in mammary tumor models. Cancer Research. 2001; 61: 7456–7463.

[9] Xin P, Pan Y, Zhu W, Huang S, Wei M, Chen C. Favorable effects of resveratrol on sympathetic neural remodeling in rats following myocardial infarction. European Journal of Pharmacology. 2010; 649: 293–300. https://doi.org/10.1016/j.ejphar.2010.09.036

[10] Feng H, Mou SQ, Li WJ, Zhang N, Zhou ZY, Ding W, et al. Resveratrol Inhibits Ischemia-Induced Myocardial Senescence Signals and NLRP3 Inflammasome Activation. Oxidative Medicine and Cellular Longevity. 2020; 2020: 2647807. https://doi.org/10.1155/2020/2647807

[11] Liu J, Zhang M, Qin C, Wang Z, Chen J, Wang R, et al. Resveratrol Attenuate Myocardial Injury by Inhibiting Ferroptosis *Via* Inducing KAT5/GPX4 in Myocardial Infarction. Frontiers in Pharmacology. 2022; 13: 906073. https://doi.org/10.3389/fphar.2022.906073

[12] Zou LX, Chen C, Yan X, Lin QY, Fang J, Li PB, et al. Resveratrol Attenuates Pressure Overload-Induced Cardiac Fibrosis and Diastolic Dysfunction via PTEN/AKT/Smad2/3 and NF-κB Signaling Pathways. Molecular Nutrition & Food Research. 2019; 63: e1900418. https://doi.org/10.1002/mnfr.201900418

[13] Arafa MH, Mohammad NS, Atteia HH, Abd-Elaziz HR. Protective effect of resveratrol against doxorubicin-induced cardiac toxicity and fibrosis in male experimental rats. Journal of Physiology and Biochemistry. 2014; 70: 701–711. https://doi.org/10.1007/s13105-014-0339-y

[14] Faul F, Erdfelder E, Buchner A, Lang AG. Statistical power analyses using G*Power 3.1: tests for correlation and regression analyses. Behavior Research Methods. 2009; 41: 1149–1160. https://doi.org/10.3758/BRM.41.4.1149

[15] Charan J, Kantharia ND. How to calculate sample size in animal studies? Journal of Pharmacology & Pharmacotherapeutics. 2013; 4: 303–306. https://doi.org/10.4103/0976-500X.119726

[16] Chin YE, Kitagawa M, Su WC, You ZH, Iwamoto Y, Fu XY. Cell growth arrest and induction of cyclin-dependent kinase inhibitor p21 WAF1/CIP1 mediated by STAT1. Science (New York, N.Y.). 1996; 272: 719–722. https://doi.org/10.1126/science.272.5262.719

[17] Gao X, Xu YX, Janakiraman N, Chapman RA, Gautam SC. Immunomodulatory activity of resveratrol: suppression of lymphocyte proliferation, development of cell-mediated cytotoxicity, and cytokine production. Biochemical Pharmacology. 2001; 62: 1299–1308. https://doi.org/10.1016/s0006-2952(01)00775-4

[18] Malaguarnera L. Influence of Resveratrol on the Immune Response. Nutrients. 2019; 11: 946. https://doi.org/10.3390/nu11050946

[19] Zhou Y, Zeng Y, Wang R, Pang J, Wang X, Pan Z, et al. Resveratrol Improves Hyperuricemia and Ameliorates Renal Injury by Modulating the Gut Microbiota. Nutrients. 2024; 16: 1086. https://doi.org/10.3390/nu16071086

[20] Wang P, Li D, Ke W, Liang D, Hu X, Chen F. Resveratrol-induced gut microbiota reduces obesity in high-fat diet-fed mice. International Journal of Obesity (2005). 2020; 44: 213–225. https://doi.org/10.1038/s41366-019-0332-1

[21] Becker SL, Manson JE. Menopause, the gut microbiome, and weight gain: correlation or causation? Menopause (New York, N.Y.). 2020; 28: 327–331. https://doi.org/10.1097/GME.0000000000001702

[22] Tsai SH, Lin-Shiau SY, Lin JK. Suppression of nitric oxide synthase and the down-regulation of the activation of NFkappaB in macrophages by resveratrol. British Journal of Pharmacology. 1999; 126: 673–680. https://doi.org/10.1038/sj.bjp.0702357

[23] Bi XL, Yang JY, Dong YX, Wang JM, Cui YH, Ikeshima T, et al. Resveratrol inhibits nitric oxide and TNF-alpha production by lipopolysaccharide-activated microglia. International Immunopharmacology. 2005; 5: 185–193. https://doi.org/10.1016/j.intimp.2004.08.008

[24] Becerril S, Rodríguez A, Catalán V, Ramírez B, Unamuno X, Portincasa P, et al. Functional Relationship between Leptin and Nitric Oxide in Metabolism. Nutrients. 2019; 11: 2129. https://doi.org/10.3390/nu11092129

[25] Abolfazli S, Karav S, Johnston TP, Sahebkar A. Regulatory effects of resveratrol on nitric oxide signaling in cardiovascular diseases. Pharmacological Reports : PR. 2025; 77: 355–374. https://doi.org/10.1007/s43440-025-00694-w

[26] Yu B, Qin SY, Hu BL, Qin QY, Jiang HX, Luo W. Resveratrol improves CCL4-induced liver fibrosis in mouse by upregulating endogenous IL-10 to reprogramme macrophages phenotype from M(LPS) to M(IL-4). Biomedicine & Pharmacotherapy = Biomedecine & Pharmacotherapie. 2019; 117: 109110. https://doi.org/10.1016/j.biopha.2019.109110

[27] Zhang P, Fang Z, Zhao M, Yi B, Huang Y, Yang H, et al. Ethanol extract of Pueraria lobata improve acute myocardial infarction in rats via regulating gut microbiota and bile acid metabolism. Phytotherapy Research : PTR. 2023; 37: 5932–5946. https://doi.org/10.1002/ptr.8005

[28] Kuch B, Muscholl M, Luchner A, Döring A, Riegger GA, Schunkert H, et al. Gender specific differences in left ventricular adaptation to obesity and hypertension. Journal of Human Hypertension. 1998; 12: 685–691. https://doi.org/10.1038/sj.jhh.1000689

[29] Krumholz HM, Larson M, Levy D, et al. Sex differences in cardiac adaptation to isolated systolic hypertension. The American Journal of Cardiology. 1993; 72: 310–3. https://doi.org/10.1016/0002-9149(93)90678-6

[30] Kobylka P, Kucinska M, Kujawski J, Lazewski D, Wierzchowski M, Murias M. Resveratrol Analogues as Selective Estrogen Signaling Pathway Modulators: Structure-Activity Relationship. Molecules (Basel, Switzerland). 2022; 27: 6973. https://doi.org/10.3390/molecules27206973

[31] van Duursen MBM. Modulation of estrogen synthesis and metabolism by phytoestrogens *in vitro* and the implications for women's health. Toxicology Research. 2017; 6: 772–794. https://doi.org/10.1039/c7tx00184c

[32] Mgbonyebi OP, Russo J, Russo IH. Antiproliferative effect of synthetic resveratrol on human breast epithelial cells. International Journal of Oncology. 1998; 12: 865–869.

[33] Levenson AS, Gehm BD, Pearce ST, Horiguchi J, Simons LA, Ward JE, 3rd, et al. Resveratrol acts as an estrogen receptor (ER) agonist in breast cancer cells stably transfected with ER alpha. International Journal of Cancer. 2003; 104: 587–596. https://doi.org/10.1002/ijc.10992

[34] Bilotta S, Arbogast J, Schart N, Frei M, Lorentz A. Resveratrol Treatment Prevents Increase of Mast Cells in Both Murine OVA Enteritis and IL-$10^{-/-}$ Colitis. International Journal of Molec-

ular Sciences. 2022; 23: 1213. https://doi.org/10.3390/ijms23031213

[35] Mödl B, Moritsch S, Zwolanek D, Eferl R. Type I and II interferon signaling in colorectal cancer liver metastasis. Cytokine. 2023; 161: 156075. https://doi.org/10.1016/j.cyto.2022.156075

[36] Yang H, Khan S, Sun A, Bai Q, Cheng H, Akhtari K. Enhancement of interferon gamma stability as an anticancer therapeutic protein against hepatocellular carcinoma upon interaction with calycosin. International Journal of Biological Macromolecules. 2021; 185: 813–820. https://doi.org/10.1016/j.ijbiomac.2021.06.159

[37] Yamaguchi H, Hiroi M, Ohmori Y. Silencing of the interferon-inducible gene Ifi204/p204 induces resistance to interferon-γ-mediated cell growth arrest of tumor cells. Cytokine. 2019; 118: 80–92. https://doi.org/10.1016/j.cyto.2018.06.029

[38] Lee JW, Oh JE, Rhee KJ, Yoo BS, Eom YW, Park SW, et al. Co-treatment with interferon-γ and 1-methyl tryptophan ameliorates cardiac fibrosis through cardiac myofibroblasts apoptosis. Molecular and Cellular Biochemistry. 2019; 458: 197–205. https://doi.org/10.1007/s11010-019-03542-7

[39] Gal R, Deres L, Toth K, Halmosi R, Habon T. The Effect of Resveratrol on the Cardiovascular System from Molecular Mechanisms to Clinical Results. International Journal of Molecular Sciences. 2021; 22: 10152. https://doi.org/10.3390/ijms221810152

[40] Bromberg JF, Horvath CM, Wen Z, Schreiber RD, Darnell JE, Jr. Transcriptionally active Stat1 is required for the antiproliferative effects of both interferon alpha and interferon gamma. Proceedings of the National Academy of Sciences of the United States of America. 1996; 93: 7673–7678. https://doi.org/10.1073/pnas.93.15.7673

[41] Fan S, Hu Y, You Y, Xue W, Chai R, Zhang X, et al. Role of resveratrol in inhibiting pathological cardiac remodeling. Frontiers in Pharmacology. 2022; 13: 924473. https://doi.org/10.3389/fphar.2022.924473

[42] Jo WS, Kim SD, Jeong SK, Oh SJ, ParK MT, Lee CG, et al. Resveratrol analogue, HS-1793, inhibits inflammatory mediator release from macrophages by interfering with the TLR4 mediated NF-κB activation. Food Science and Biotechnology. 2022; 31: 433–441. https://doi.org/10.1007/s10068-022-01052-9